

Kinase inhibitors can inhibit SARS-CoV-2 M^{pro}:

A Theoretical Study

Badri Narayan Acharya

Synthetic Chemistry Division

Defence R&D Establishment, Jhansi Road, Gwalior-474002

Abstract This study describes screening of DrugBank library for approved drugs by pharmacophore modeling and receptor-ligand docking. A 3D-QSAR model was generated on the inhibition constants ($K_{i\text{AutoDock}}$) determined by AutoDock. This 3D-QSAR model was statistically validated by *Fischer's* randomization test and further evaluated by a test set comprising 75 molecules. $K_{i\text{AutoDock}}$ values of 49 molecules were predicted correctly by the 3D-QSAR model. The validated 3D-QSAR model was used for screening of DrugBank library for approved molecules to identify potential molecules against novel SARS corona virus-2 (SARS CoV-2). Ten out of 40 the shortlisted molecules were kinase inhibitors.

Keywords Pharmacophore • COVID-19 • M^{pro} • Docking • Kinase Inhibitors

✉ Badri Narayan Acharya

bnacharya@yahoo.com

Defence R&D Establishment, Jhansi Road, Gwalior, India

Introduction

The Global pandemic of novel corona virus disease 2019 (COVID-19) caused by severe acute respiratory syndrome coronavirus 2 (SARS-CoV-2) [1]. COVID-19 pandemic has become most severe global public health crisis since the pandemic influenza outbreak of 1918. As of July 3, 2020, there have been more than 10.5 million reported cases and more than 512,800 deaths in more than 200 countries. In India more than 604,000 cases infection and 17,834 deaths are recorded in same period of time. In a recent review, sanders et al, summarizes regarding major proposed treatments, repurposed or experimental for COVID-19 [2]. In emergency *Favipiravir* has been introduced in India for management of COVID-19 pandemic.

COVID-19 virus genome is comprised of ~30,000 nucleotides encodes two overlapping poly proteins required for viral replication and transcription [3]. The functional proteins are released by extensive proteolysis of the polyproteins by a 33.8 kDa main protease (M^{pro}) [4]. The function of viral M^{pro} in the life cycle of the virus and absence of similar protease in humans makes it an automatic choice for antiviral drug target [4]. Structure-based drug designing (SBDD) is an effective tool for discovery of potential bioactive molecules. Based on the receptor structure, effective inhibitors can be designed. Recently Jin et al have reported the structure of M^{pro} co-crystallized with an inhibitor N3 by x-ray crystallography [5]. SBDD can be used to facilitate rapid discovery of antiviral drug compounds with clinical potential by repurposing existing drugs to target COVID-19 virus M^{pro} [6].

In a previous work [7], a common feature pharmacophore model generated on six M^{pro} inhibitors identified by Jin et.al with IC_{50} values of enzyme inhibition in the range of 0.67 to 21.4 μM [5]. NCI 2000 database was screened by the pharmacophore model and *Amodiaquine* was identified as a potential M^{pro} inhibitor [7]. The M^{pro} inhibition constant ($K_{i\text{Docking}}$) of

Amodiaquine was determined by receptor-ligand molecular docking. Two stage screening may be effective to identify potential molecules but a quick predictive tool like 3D-QSAR would be more effective to rank and priorities the molecules for next level of testing.

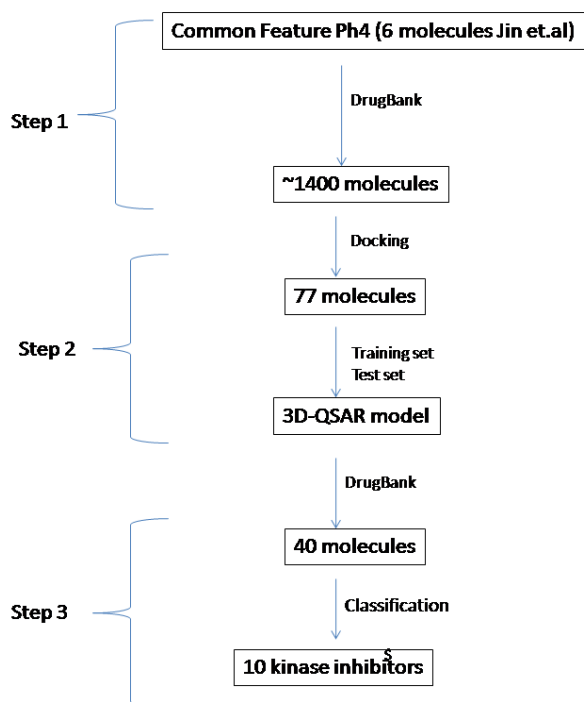


Fig 1. Three step approach for screening

In this work, a three step approach (Fig 1) has been adopted to screen several drug molecules as potential repurposing drugs for COVID-19 from DrugBank data base [8]. DrugBank database for approved drugs contains 2,635 molecules. In first step the pharmacophore model [7] screened ~1400 molecules which contain the minimum pharmacophoric features required to inhibit M^{pro} . In the second step, top 77 molecules were docked with M^{pro} and $K_{i\text{Docking}}$ were calculated by receptor-ligand docking simulation. These 77 molecules were divided in to training set and test set molecules. A 3D-QSAR model was generated based on $K_{i\text{Docking}}$ of a training set comprising 16 molecules. The generated 3D-QSAR model was validated by Fischer's randomization test for

statistical significance. The most statistically significant model was used to predict the $K_{i\text{Docking}}$ values of a test set comprising 75 molecules including some of the training set molecules. This 3D-QSAR model was used to screen DrugBank database for approved drugs. In return 106 molecules were obtained out of which 40 molecules showed K_i value under 1 μM . Ten out of 40 molecules were found different types of kinase inhibitors primarily used as anticancer drugs.

Materials and Methods

Pharmacophore modeling

Pharmacophore hypotheses were generated as described before [7] using Catalyst HipHop algorithm as present in DiscoveryStudioTM 2.0 [9]. In brief, training set molecules shown in Fig 2a were drawn and geometry optimized. Input parameters include features hydrogen bond donor (HBD), hydrogen bond acceptor (HBA), positive ionizable (PI), hydrophobe (HY) and ring aromatic (RA), maximum 10 and minimum 1 features, minimum inter feature distance 2.97 Å, maximum conformations 255, energy threshold 20 kcal/mol. Poling algorithm was used to generate conformations for each molecule in ‘fast mode’. HipHop conducts an exhaustive search starting with the simplest to more complicated pharmacophores. The process continues until common pharmacophore combinations can no longer be generated. The final HipHop output was top ten unique pharmacophores sorted from highest to lowest scoring. Then the top ranked hypothesis was used to screen DrugBank databases to shortlist potential molecules [8].

Docking Studies

Structures of M^{PRO} of COVID-19 virus (pdb id: 6lu7) [5] was downloaded from protein data bank and used for receptor-ligand interaction studies as described before [7]. In brief, structure was cleaned from water and ligand molecules coded as N3. The protein contains many binding pockets in its structure as identified by inbuilt method of DiscoveryStudioTM 2.0. The pocket closer to catalytic aminoacid CYS 145 was identified having the central coordinates at -12.12, 13.884, 64.03. The cleaned structure of M^{PRO} was imported to MGLTools-1.5.4 [10] for preparation of docking studies. HIS 164 of M^{PRO} was selected as flexible residue. Docking studies were carried out by AutoDock 4.1 [10]. For docking of inhibitors with M^{PRO}, grid center was set at -12.12, 13.884, and 64.03. Number of grid points in each direction was 40 and grids were generated for each ligands before docking. Ligands shortlisted from pharmacophore screening were prepared with Gastegier's charges at prescribed torsions. Lamarckian Genetic Algorithm (LGA) was used for conformation generation and determination of best interactions between receptor and ligand. Seed population was 150, number of evaluations was 2,500,000, and number of generation was set at 27000. Rate of mutation and crossover were 0.02 and 0.8 respectively. Top ten conformations were returned after each run. Binding energy (kcal/mol) and predicted inhibition constant (K_i) were recorded.

Generation of 3D-QSAR model

3D-QSAR model was generated by HypoGen module of Discovery StudioTM. In this work, 3D-QSAR model is generated on the basis of $K_{i\text{Docking}}$ values (nM) of different DrugBank molecules shortlisted by common feature pharmacophore model. Molecules with lower $K_{i\text{Docking}}$ values were treated as more active for inhibition of M^{PRO}. HypoGen requires both active and inactive molecules in a training set to generate meaningful pharmacophore hypotheses. Selection of

training set follows some basic requirements, such as selecting a minimum of 16 structurally diverse compounds to avoid any chance of correlation [11]. The training set was chosen in such a way that it contained both active and inactive molecules covering an activity range of 5 orders. Input parameters include features hydrogen bond donor (HBD), hydrogen bond acceptor (HBA), positive ionizable (PI), hydrophobe (Hy) and ring aromatic (RA), maximum 10 and minimum 1 features, minimum inter feature distance 2.97 Å, maximum conformations 255, energy threshold 20 kcal/mol and maximum excluded volume 100. Poling algorithm was used to generate conformations for each molecule in 'fast mode'. The value of uncertainties in biological data is also a crucial parameter to differentiate the active molecules from the inactive molecules based on a very simple calculation. First the activity of the most active compound is multiplied with its corresponding uncertainty to establish a benchmark number. The activity of other compounds in the training set were divided by their respective uncertainties and compared. If the value is less than the benchmark number, then the compound is considered as active else inactive. HypoGen follows three steps to generate pharmacophore hypotheses; they are constructive, subtractive and optimization. In the constructive phase all the pharmacophores of the active molecules are pulled. In the subtractive phase those pharmacophores are deleted which are present in the inactive molecules. In the optimisation phase predictability of the hypothesis is optimized with complexity. When optimization no longer improves the cost function score, generation of new hypothesis stops [11].

Cost analysis

The HypoGen module of DiscoveryStudio performs three important cost calculations in the units of bits that determine the success of any pharmacophore hypotheses: 'fixed cost', which represents the simplest model that fits all data perfectly; 'null cost', which represents the highest

cost of a pharmacophore with no features and estimates activity to be the mean of the activity data of the training set molecules. Its absolute value is equal to the maximum occurring error cost. A meaningful pharmacophore hypothesis may result when the difference between these two values (null cost minus total cost) is greater than 20, 'total cost' is the sum of three cost factors: a weight, an error, and a configuration cost. The weight cost increases if the weight factor for the chemical features deviate from the default value of 2. The error cost is solely dependent on the root-mean-square (rms) differences between the estimated and actual activities of the training set molecules. The rms value represents the quality of the correlation between the actual and the estimated activity data. The configuration cost is represented as Log_2P , where P is the number of initial hypotheses created in the constructive phase and that survived in the subtractive phase [11].

Fischer's randomization test and validation

To evaluate the statistical relevance of the models, Fisher's randomization test was applied. The purpose of this test is to randomize the activity data associated with the training set. The randomized training sets are used to generate hypotheses using the same features and parameters. If the randomized data sets result in the generation of pharmacophores with similar or better cost values, rms, and correlation the original hypothesis is considered to have been generated by chance. The statistical significance is given by the equation of significance = $[1-(1+x)/y]$, where x is the total number of hypotheses having total cost lower than the most-significant hypothesis and y is the number of initial HypoGen runs plus random runs. With the aid of the CatScramble program available in the HypoGen module, the activities of the molecules in the training set were randomized and the resulting training sets were used for the HypoGen runs. In this way all parameters were kept as per the initial HypoGen calculation. Finally, the biological activities of

the test set molecules were predicted to check the predictive ability of the generated hypotheses [11].

Results and Discussion

Generation of pharmacophore model

Jin et.al [5] screened ~10,000 compounds consisting of approved drugs, drug candidates in clinical trials and natural products by fluorescence resonance energy transfer (FRET) assay. Six compounds namely *Ebselen*, *Tideglusib*, *Shikonin*, *Disulfiram*, *Carmofur*, and *PX-12* were found as hits in the FRET assay and their IC₅₀ values were found in between 0.67 to 21.4 μ M concentration. Common feature pharmacophore modeling [11] requires structure of active molecules to identify and enumerate all possible pharmacophore configurations which in common within the training set molecules.

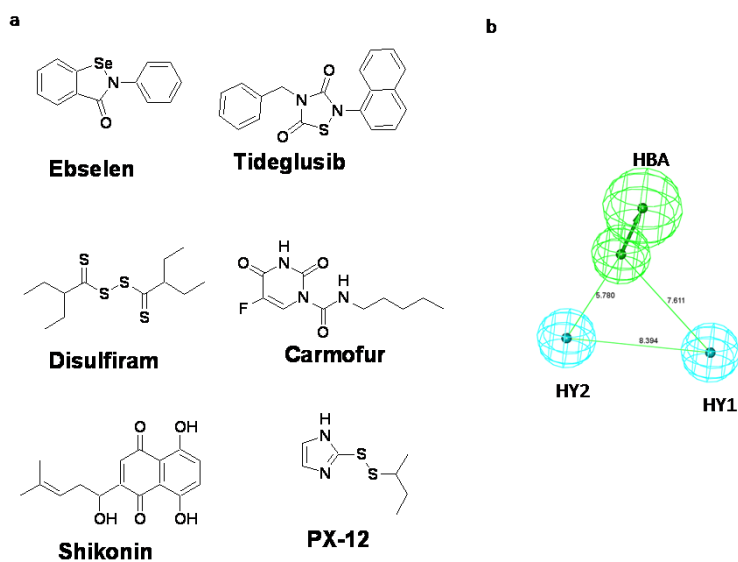


Fig.2 Training set molecules (a); pharmacophore model (b)

These six molecules (Fig 2a) were taken in the training set to generate common feature pharmacophore models as described in the materials and methods. In this process, a three feature pharmacophore model containing one HBA (hydrogen bond acceptor) and two HY (hydrophobe)

was obtained (Fig 2b). The distances between HBA-HY1, HBA-HY2 and HY1-HY2 are 7.611, 5.780 and 8.3 Å respectively.

Virtual screening of DrugBank database

DrugBank database (version 5.1.6) is a unique resource of drug entities including 2,635 approved small molecule drugs [8]. The approved drug molecules were downloaded and integrated to DiscoveryStudio 2.0 as a virtual library. DiscoveryStudio 2.0 built multiple conformations of each drug molecule and stored them in the virtual library. This DrugBank library was screened by the pharmacophore model and in return 1,403 molecules were obtained. These 1,403 molecules contain minimum pharmacophores to bind with M^{pro} catalytic site, but the actual binding may be affected due to presence of other features and configurations present in the molecules. Hence all the molecules should be docked in the catalytic site of M^{pro} to determine the inhibition constant ($K_{i\text{Docking}}$). But docking all these molecules will take a long time with AutoDock. Hence a three dimensional quantitative structure activity relationship (3D-QSAR) model was developed to quickly estimate the inhibition constant ($K_{i\text{3D-QSAR}}$) of different drug molecules against M^{pro} which must have reasonable correlation with $K_{i\text{Docking}}$. DrugBank was screened by the 3D-QSAR model to shortlist and rank molecules with respect to their theoretical activities.

Development of 3D-QSAR model

The 1,403 molecules screened by pharmacophore model were sorted by their fit values. Seventy seven molecules were considered for ligand-receptor interaction studies by AutoDock (Fit values and $K_{i\text{Docking}}$ values are given in supplementary material, Table S1). Sixteen molecules (Fig 3) from them were selected as training set to generate the 3D-QSAR model as described in materials and methods top 10 hypotheses were exported (Table 1). Netrolone phenopropionate

(DB00984) was excluded from training set because it significantly lowered the correlation (r) value of the hypotheses although it had shown the best $K_{iDocking}$ value (0.83 nM).

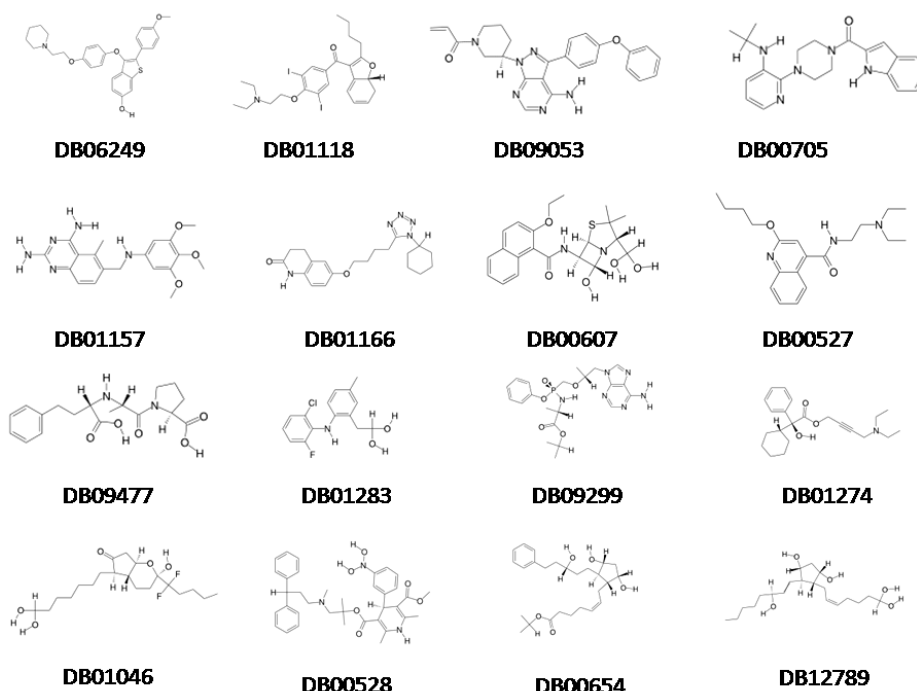


Fig 3. Training set molecule for 3D-QSAR model

Table 1. Results of top 10 pharmacophore hypotheses generated using training set (Fig.3)

Hypotheses	Total Cost	Cost Difference ^a	RMS ^b	Correlation (r)	Features ^c	Significance ^d
1	81.014	21.82	0.978	0.919	Hy,Hy,PI,RA	80%
2	81.953	20.88	1.020	0.912	Hy,Hy,PI,RA	90%
3	82.436	20.40	1.084	0.898	Hy,Hy,PI,RA	90%
4	82.647	20.19	1.098	0.896	Hy,Hy,PI,RA	95%
5	86.045	16.79	1.250	0.864	Hy,Hy,PI,RA	95%
6	86.063	16.77	1.202	0.879	Hy,Hy,RA,HBA	95%
7	86.434	16.40	1.275	0.858	Hy,Hy,RA,HBA,PI	95%
8	86.849	15.99	1.315	0.847	HBA,Hy,PI,RA	95%
9	87.264	15.57	1.294	0.853	Hy,PI,RA,RA	95%
10	87.343	15.49	1.264	0.865	Hy,Hy,RA,HBA	95%

^aCost Difference = null cost-total cost. Null cost=102.834. Fixed cost=72.99. Configuration cost=18.075.

^bRMS, root mean square deviation of the AutoDock estimated K_i and 3D-QSAR estimated K_i .

^cHy: Hydrophobe, PI: Positive ionisable, RA:Ring aromatic, HBA: Hydrogen bond acceptor

^dSignificance at confidence level 95% (from randomization test)

All of the hypotheses showed correlation in the range of 0.865 to 0.919 which is considerable in case of a quantitative structure activity relationship (Table 1). The RMS values were also not very high which indicates a good agreement in between $Ki_{3D-QSAR}$ and $Ki_{Docking}$ values. Most of the hypotheses showed Hy, Hy, PI and RA as primary features. Hypothesis 6, 7 and 10 have HBA feature. Hypothesis 7 has five features, the maximum among 10 hypotheses.

To further evaluate the statistical relevance of the model, Fischer's randomization test was applied. In this process the input training set was scrambled randomly and the resulting training sets were subjected to pharmacophore generation. This process was repeated 19 times to achieve a confidence limit of 95%. Interestingly, top three hypotheses showed lower significance values compared to hypotheses 4 to 10 (Table 1). This may be due to the nature of $Ki_{Docking}$ values which were estimated theoretically by AutoDock rather generated experimentally. Currently very little experimental information is available regarding Ki of different small molecules against M^{pro} .

Hypotheses 4 to 10 returned by HypoGen passed randomization test which indicates that the hypotheses are meaningful and they are not generated by chance (Table 1). Based on randomization test and cost values, 'hypothesis 4' was selected as best hypothesis for 3D-QSAR model. Hypothesis 4 has four features (Fig. 3a): one positive ionisable (PI), one ring-aromatic (RA) and two hydrophobes (Hy). The fixed cost, total cost and null cost for hypothesis 4 are 72.99, 82.64 and 102.83 respectively. The difference between Total cost and fixed cost is 9.65. This is significantly lower than the difference between null cost and total cost (20.19). The high correlation coefficient and low rms values of 0.89 and 1.09 respectively indicate that the generated model is statistically significant. The $Ki_{Docking}$ and $Ki_{3D-QSAR}$ values of all 16 training set molecules are given in Table 2. Molecules mapped with Hypothesis 4 are shown in Fig 4.

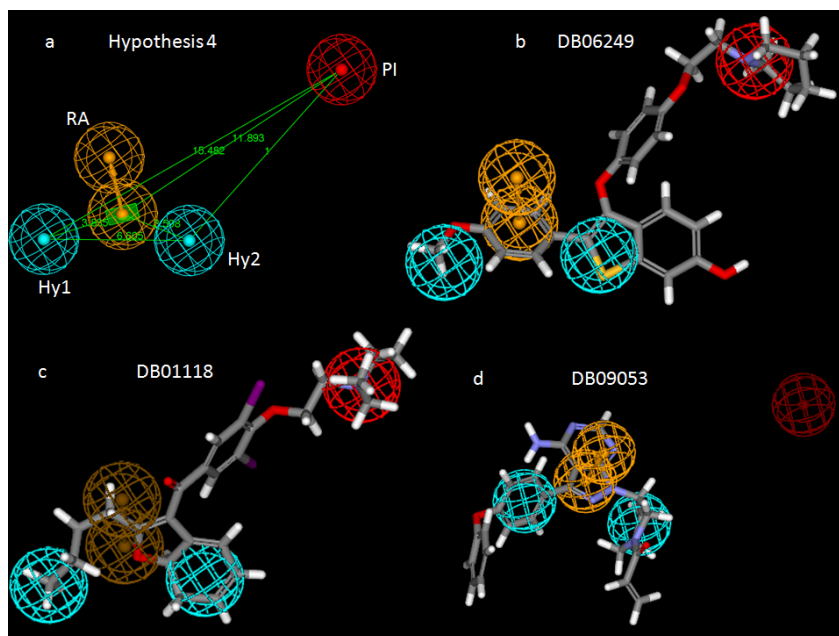


Fig 4. 3D-QSAR model ‘hypothesis 4’ (a); Molecules mapped on hypothesis 4 DB06249 (b), DB01118(c), DB09053 (d).

Table 2. $K_{i\text{Docking}}$ and $K_{i3\text{D-QSAR}}$ values of training set molecules calculated by hypothesis 4.

Sl no	DrugBank ID	Fit	IC ₅₀ (nM) ^a		Activity scale ^a		Erro r	Features mapped ^b
			$K_{i\text{Docking}}$	$K_{i3\text{D-QSAR}}$	$K_{i\text{Docking}}$	$K_{i3\text{D-QSAR}}$		
1	DB06249	7.31	3	2.3	+++	+++	- 1.3	Hy, Hy, PI, RA
2	DB01118	5.99	3.5	48	+++	++	+ 14	Hy, Hy, PI, --
3	DB09053	5.93	15	55	++	++	+ 3.8	Hy, Hy, --, RA
4	DB00705	5.69	45	96	++	++	+ 2.1	Hy, Hy, --, RA
5	DB01157	6.00	75	47	++	++	- 1.6	Hy, Hy, --, RA
6	DB01166	5.98	100	49	++	++	- 2.1	Hy, Hy, --, RA
7	DB00607	5.44	250	170	++	++	- 1.5	Hy, Hy, --, RA
8	DB00527	5.86	450	64	++	++	- 7	Hy, Hy, --, RA
9	DB09477	4.01	680	4600	++	+	+ 6.7	Hy, Hy, --, RA
10	DB01283	5.15	990	340	++	++	- 2.9	-- Hy, PI, RA
11	DB09299	4.41	1700	1800	+	+	+ 1.1	Hy, Hy, -- RA
12	DB01274	4.01	2700	4600	+	+	+ 1.7	Hy, Hy, --, --
13	DB01046	3.52	6600	1,40,000	+	+	+ 2.1	-- Hy, PI, RA
14	DB00528	4.01	9300	4600	+	+	- 2.4	Hy,Hy, -- , RA
15	DB00654	4.01	11000	4600	+	+	- 2.4	-- Hy, PI,RA
16	DB12789	4.01	21000	4600	+	+	- 4.6	--, Hy, PI, RA

^a Activity scale: +++ (0.1-10 nM, highly active), ++ (11-999 nM, moderately active), + (>1000 nM, poorly active)

^bHy: Hydrophobe, PI: Positive ionisable, RA:Ring aromatic, HBA: Hydrogen bond acceptor

In the randomization test, none of the resulting hypotheses were found statistically better than ‘hypothesis 4’ (Table 3). It proves that ‘hypothesis 4’ was not generated by chance. Seventy five molecules were kept in ‘test set’ for validation of 3D-QSAR model which also included some

training set molecules. Hypothesis 4 was further validated by the ‘test set’ to evaluate its predictive ability of K_i . A prediction within ten fold range of $K_{i\text{Docking}}$ was kept as a good prediction ability of the 3D-QSAR model i.e the ratio $K_{i\text{3D-QSAR}}/K_{i\text{Docking}}$ should fall within 0.1 to 10. Forty-nine out of 75 molecules in the test set were predicted well in the prescribed limit (see supplementary material Table S2, marked in yellow).

Table 3 Results from cross-validation run using CatScramble for hypothesis 4.

Hypothesis number	Total cost	Correlation (r)
Trial 1	99.96	0.627
Trial 2	82.88	0.877
Trial 3	100.01	0.679
Trial 4	91.63	0.815
Trial 5	93.29	0.796
Trial 6	93.54	0.816
Trial 7	93.35	0.780
Trial 8	91.59	0.818
Trial 9	95.08	0.736
Trial 10	96.02	0.707
Trial 11	82.74	0.886
Trial 12	94.55	0.817
Trial 13	94.14	0.737
Trial 14	91.31	0.817
Trial 15	92.10	0.828
Trial 16	101.26	0.667
Trial 17	90.81	0.835
Trial 18	93.22	0.771
Trial 19	88.68	0.852
Hypothesis 4	82.64	0.896

^a Null cost = 155.23. All costs are in bits.

The 3D-QSAR model was used to screen DrugBank database for approved drugs which contains 2635 molecules. In return 106 molecules were obtained out of which 40 molecules were detected having $K_{i\text{3D-QSAR}}$ value less than 1 μM (Table 4). The short listed molecules are approved drugs in many categories comprising anti-cholinergics, antibacterials, antimalarial, kinase inhibitors, anti arrhythmic, anti-hypertensive, antifungal and PDE5 inhibitors. The top two molecules *Mivacurium* and *Doxacurium* belong to antichlonergic drugs used as muscle relaxant. As the drugs are active on nervous system their repurposing may be problematic against COVID-19.

Isovacuonazonium is a molecule for external use and *Arzoxifene* an estrogen receptor modulator may not be appropriate for repurposing.

Table 4 Molecules screened by 3D-QSAR model with Ki value less than 1 μ M

Sl no	DrugBank ID	Name	FitValue ^a	Ki _{3D-QSAR} (nM) ^b	Remarks
1	DB01226	Mivacurium	7.763	0.808	Neuromuscular blocker
2	DB01135	Doxacurium	7.702	0.928	Skeletal muscle relaxant
3	DB06636	Isovacuonazonium	7.605	1.162	Antifungal
4	DB06249	Arzoxifene	7.313	2.274	Estrogen receptor modulator
5	DB12001	Abemaciclib	7.29	2.398	Cyclin dependent kinase (CDK) inhibitor
6	DB12141	Gilteritinib	7.081	3.878	Tyrosine kinase inhibitor
7	DB00662	Trimethobenzamide	7.024	4.427	Antiemetic
8	DB00732	Atracurium	6.785	7.67	Anticholinergic
9	DB09048	Netupitant	6.756	8.206	Antiemetic
10	DB11761	Tenapanor	6.583	12.209	IBS-C
11	DB13265	Hexobendine	6.474	15.699	Vasodilation
12	DB12267	Brigatinib	6.306	23.11	Tyrosine kinase inhibitor
13	DB06608	Tefanoquine	6.25	26.284	Antimalarial drug
14	DB00688	Epinephrine	6.106	36.625	Hormone
15	DB09079	Nintedanib	6.088	38.223	Tyrosine kinase inhibitor
16	DB06695	Debigatran	6.06	40.773	Anticoagulant
17	DB01419	Antrafenine	6.025	44.112	Anti-inflammatory
18	DB00203	Sildenafil	6.001	46.64	PDE5 inhibitor
19	DB04855	Dronedarone	5.963	50.912	Anti-arrhythmic
20	DB09374	Indocyanine	5.887	60.683	Coloring agent
21	DB00251	Terconazole	5.861	64.395	Anti-fungal
22	DB13931	Netarsudil	5.784	76.957	Rho kinase inhibitor
23	DB00416	Metocurine iodide	5.769	79.571	Muscle relaxant
24	DB01336	Metocurine	5.769	79.571	Muscle relaxant
25	DB11691	Naldemedine	5.706	91.969	Opioid receptor antagonist
26	DB12500	Fedratinib	5.272	249.87	Tyrosine kinase inhibitor
27	DB00862	Vardenafil	5.27	251.114	PDE5 inhibitor
28	DB09073	Palbociclib	5.261	256.433	Cyclin dependent kinase (CDK) inhibitor
29	DB11855	Revefenacin	5.173	314.163	Long acting muscarinic inhibitor
30	DB00619	Imatinib	5.139	340.013	Tyrosine kinase inhibitor
31	DB01180	Rescinnamine	5.124	351.333	ACE inhibitor from <i>Rauwolfia serpentina</i>
32	DB00565	Cisatacurium	5.037	429.404	Anticholinergic
33	DB11363	Alectinib	5.018	448.25	Tyrosine kinase inhibitor
34	DB04209	Dequalinium	5.001	466.542	Antiseptic and disinfectant
35	DB01089	Deserpidine	4.992	476.268	Antihypertensive and antipsychotic
36	DB01118	Amiodarone	4.952	522.892	Anti-arrhythmic
37	DB06402	Telavancin	4.849	662.519	Antibacterial
38	DB11963	Dacomitinib	4.81	723.784	Tyrosine kinase inhibitor
39	DB04911	Oritavancin	4.808	727.554	Antibiotic
40	DB06267	Udenafil	4.716	898.802	PDE5 inhibitor

^a Fit with 3D-QSAR model

^b Estimated by 3D-QSAR model

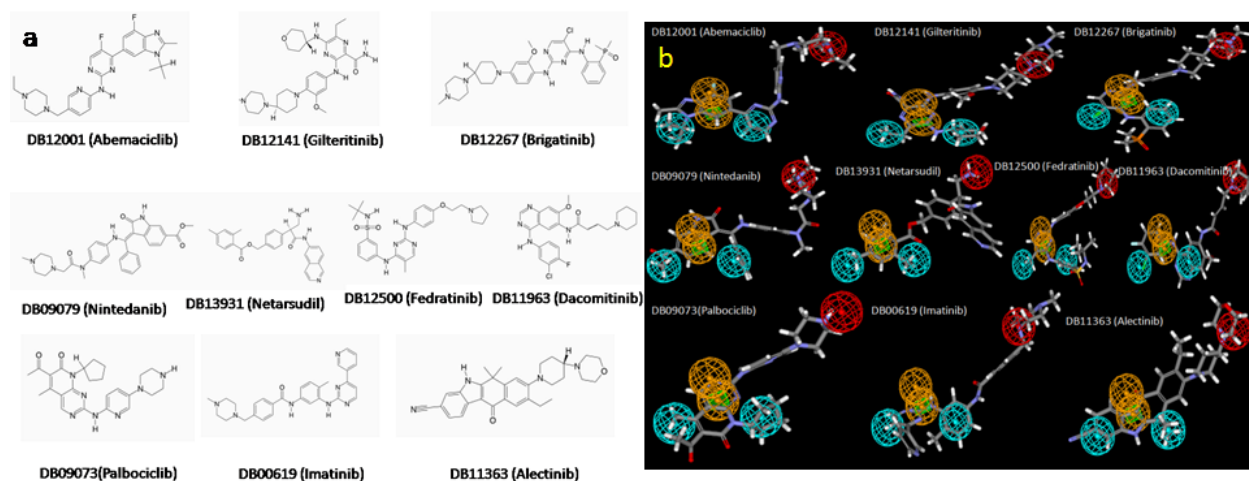


Fig 5. Kinase inhibitors screened by 3D-QSAR model (a); Mapping of the kinase inhibitors with the 3D-QSAR model (b).

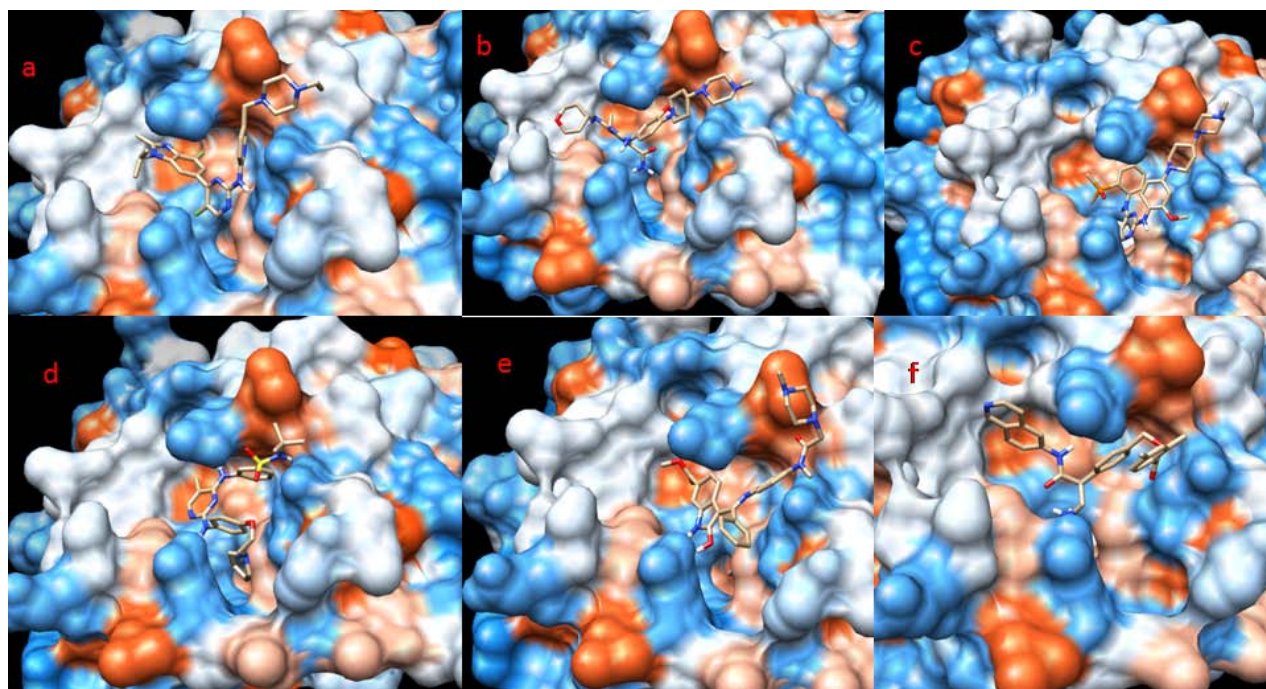


Fig 6. Kinase inhibitors docked in the active site of M^{pro} ; Abemaciclib (DB12001) (a); Gilteritinib (DB12141) (b); Brigatinib (DB12141) (c); Fedratinib (DB12141) (d); Nintedanib (DB09079) (e); Netrosudil (DB13931) (f).

Interestingly, ten molecules (Fig 5a) namely *Abemaciclib*, *Gilteritinib*, *Brigatinib*, *Nintedanib*, *Netarsudil*, *Fedratinib*, *Palbociclib*, *Imatinib*, *Alectinib* and *Dacomitinib* were short listed which are kinase inhibitors. *Netarsudil* is a Rho kinase inhibitor; *Abemaciclib* and *Palbociclib* are cyclin dependent kinase (CDK) inhibitors; rests are tyrosine kinase inhibitors. Molecules mapped with 3D-QSAR model are also shown in Fig 5b. The docking pose of some kinase inhibitors in the active site of the M^{pro} enzyme generated by UCSF Chimera [13] are shown in Fig 6. Inhibition constant (Ki) values estimated by 3D-QSAR and AutoDock are given in Table 5.

Table 5. Estimated Ki values of kinase inhibitors with M^{pro}

Sl no	DrugBank ID	Name	Ki _{3D-QSAR} (nM) ^a	Ki _{AutoDock} (nM) ^b
1	DB12001	Abemaciclib	2.398	155
2	DB12141	Gilteritinib	3.878	34
3	DB12267	Brigatinib	23.11	2.81
4	DB09079	Nintedanib	38.223	6.66
5	DB13931	Netarsudil	76.957	25.45
6	DB12500	Fedratinib	249.87	20.31
7	DB09073	Palbociclib	256.433	n.c
8	DB00619	Imatinib	340.013	n.c
9	DB11363	Alectinib	448.25	n.c
10	DB11963	Dacomitinib	723.784	41.79

^a Estimated by 3D-QSAR model; ^b Estimated by AutoDock; n.c not calculated

Schor and Einav [12] have elaborately discussed about various kinase inhibitors which can be repurposed as broad spectrum antivirals. Kinase inhibitors target host cell mechanisms and impart antiviral activity indirectly. These molecules can act against many viruses because viruses use cell machinery for their replication. In the current work it has been observed that many of the kinase inhibitors can inhibit M^{pro} enzyme of SARS CoV-2, hence can act as direct acting antiviral agents (DAAs).

Conclusion

3D-QSAR is an effective tool to identify potential inhibitor for COVID-19 M^{pro}. Due to lack of enough experimental data above model was generated from theoretical inhibition constants ($K_{i\text{Docking}}$) generated by AutoDock. With statistical significance, this model was used to screen DrugBank database for approved drugs. Different categories of drug molecules were screened but kinase inhibitors were appeared more in the screening. Kinase inhibitors are known to show broad spectrum antiviral activity by targeting host cell machinery. But in this study, through molecular modeling it is hypothesized that they can show activity against COVID-19 by inhibiting M^{pro} enzyme of the target virus. Hence more work should be carried out to establish the direct antiviral activity of kinase inhibitors and the effective molecules may be repurposed against COVID-19.

Acknowledgement

Authors are thankful to the Director DRDE Gwalior for necessary support and advice during this work. The manuscript is assigned DRDE accession no. DRDE/SC/10/2020.

Conflict of interests

None

References

1. Zhu N, Zhang D, Wang W et al (2020) New Engl J Med 382 (8):727-733
2. Sanders JM, Monogue ML, Jodlowski TZ, Cutrell JB (2020) JAMA doi:10.1001/jama.2020.6019.
3. a. Zhou P et al. (2020) Nature 579:270
4. Wu F et al. (2020) Nature 579:265
5. Jin Z, Du X, Xu Y, Deng Y, Liu M, Zhao Y, Zhang B, Li X, Zhang X, Peng C, Duan Y, Yu J, Wang L, Yang K, Liu F, Jiang R, Yang X, You T, Liu X, Yang X, Bai F, Liu H, Liu X,

- Guddat LW, Xu W, Xiao G, Qin C, Shi Z, Jiang H, Rao Z, Yang H (2020) Nature doi:10.1038/s41586-020-2223-y
6. Smith M, Smith JC (2020) ChemRxiv doi.org/10.26434/chemrxiv.11871402.v4
 7. Acharya BN (2020) CHEMRxiv doi.org/10.26434/chemrxiv.12555137.v1
 8. Wishart DS, Feunang YD, Guo AC, LoEJ, Marcu A, Grant JR, Sajed T, Jonson D, Li C, Sayeeda Z, Assempour N, Iyankaran I, Liu Y, Maciejewski A, Gale N, Wilson A, Chin L, Cummings R, Le D, Pon A, Knox C, Wilson M (2017) Nucleic Acids res Nov 8 Doi: 10.1093/nar/gkx1037
 9. Accelrys, Inc. Discovery Studio, version 2.0 (2007) San Diego, CA
 10. Morris GM, Huey R, Lindstorm W, Sanner MF, Belew RK, Goodshell DS, Olson AJ (2009) J Compu Chem 16: 2785
 11. Kurogi Y, Güner OF (2001) Curr Med Chem 8: 1035
 12. Schors S, Einav S (2018) DNA Cell Biol 37(2): 63-69
 13. Pettersen EF, Goddard TD, Huang CC, Couch GS, Greenblatt DM, Meng EC, Ferrin TE. (2004) J Comput Chem. 25(13):1605-1612